Optical modulation of excitation-contraction coupling in human induced pluripotent stem cell-derived cardiomyocytes

Vito Vurro[a], Beatrice Federici[a], Carlotta Ronchi[a], Valentina Sesti[a,b], Silvia Crasto[c,d,#], Claudia Maniezzi[e], Maria Rosa Antognazza[a], Chiara Bertarelli[a,b], Elisa Di Pasquale[c,d], Guglielmo Lanzani[a,f,*], Francesco Lodola[a,e,*]

[a]Center for Nano Science and Technology @PoliMi, Istituto Italiano di Tecnologia, Via Pascoli 70/3, 20133, Milan, Italy;

[b]Department of Chemistry, Materials and Engineering Chemistry 'Giulio Natta', Politecnico di Milano, Piazza Leonardo da Vinci, 32, 20133, Milan, Italy;

[c]Institute of Genetic and Biomedical Research (IRGB), UOS of Milan, National Research Council of Italy, 20138, Milan, Italy;

[d]Department of Cardiovascular Medicine, Stem Cells Laboratory Humanitas Clinical and Research Center-IRCCS, 20089, Rozzano (MI), Italy;

[e]Department of Biotechnology and Biosciences, University of Milan-Bicocca, Building U3, Piazza della Scienza, 2, 20126, Milan, Italy;

[f]Department of Physics, Politecnico di Milano, Piazza Leonardo da Vinci, 32, 20133, Milan, Italy.

Corresponding authors: Francesco Lodola (francesco.lodola@unimib.it); Guglielmo Lanzani (guglielmo.lanzani@iit.it)

Present address: Amarin Italy S.r.l., Corso Vercelli 40, 20145, Milan, Italy.

Abstract

Non-genetic photostimulation is a novel and rapidly growing multidisciplinary field of research that aims to induce light sensitivity in living systems by exploiting exogeneous phototransducers.

Here we propose a recently synthetized intramembrane photo-transducer, based on an azobenzene derivative (Ziapin2), for optical pacing of human induced pluripotent stem cell-derived cardiomyocytes (hiPSC-CMs).

The light-mediated photostimulation process has been studied by applying a number of characterization techniques to detect the effect on the cell properties. In particular, we recorded changes in membrane capacitance, in membrane potential (V_m), and modulation of intracellular Ca^{2+} dynamics. Finally, cell contractility was analyzed using a custom MATLAB algorithm.

Photostimulation of intra-membrane Ziapin2 causes a transient V_m hyperpolarization followed by a delayed depolarization and action potential firing. The observed initial electrical modulation nicely correlates with changes in Ca^{2+} dynamics and contraction rate.

This work represents the proof of principle that Ziapin2 is able to modulate electrical activity and contractility in hiPSC-CMs, opening up a future development in cardiac electrophysiology.

Keywords: light stimulation, molecular photoswitches, nanoactuators, hiPSC-CMs optical pacing, cardiac cell modulation

1. Introduction

In the cardiovascular field, optical stimulation is emerging as an alternative to traditional approaches for many research and therapeutic applications thanks to a series of key-enabling features: the lower energy consumption and release, minimal invasiveness net of an extraordinary spatial and temporal resolution (Antognazza et al., 2015; Di Maria et al., 2018; Hopkins et al., 2019).

Optogenetics (Deisseroth, 2011; Fenno et al., 2011; Rein and Deussing, 2012; Deisseroth, 2015; Duebel et al., 2015; Dwenger et al., 2019), that has been successfully used in neuroscience, could in principle be relevant in the cardiac field too (Knollmann, 2010; Bruegmann et al., 2010; Ambrosi et al., 2014; Boyle et al., 2018; Asano et al., 2018; Ferenczi et al., 2019; Sasse et al., 2019; Krueger et al., 2019; Huang et al., 2020; Floria et al., 2020; Li et al., 2021; Crocini et al., 2016; Biasci et al., 2022). However, the approach still has a limited clinical applicability mainly because cell optical sensitivity is obtained by transduction with gene constructs carried by viral vectors.

A possible alternative strategy to overcome these constraints relies on the use of light-sensitive transducers, based on both inorganic and organic semiconductors (Starovoytov et al., 2005; Bareket-Keren and Hanein, 2014; Savchenko et al., 2018; Rand et al., 2018; Feiner and Dvir, 2019; Francesco Lodola et al., 2019; Parameswaran et al., 2019; Bruno et al., 2021; F Lodola et al., 2019; Negri et al., 2022). Those have been used recently as photoactive interfaces for cardiomyocyte (CMs) optical stimulation. The generation of action potentials (APs) has been demonstrated by using planar graphene-based biointerfaces, possibly exploiting the photogeneration of charge carriers, and with polymer-silicon nanowires utilizing their photoelectrochemical properties (Parameswaran et al., 2019; Savchenko et al., 2018). Similar results were obtained also increasing the local temperature with illumination of absorbers in contact with CMs, using gold nanoparticles or nanorod electrodes and metasurface planar organic interfaces (Bruno et al., 2021; Fang et al., 2022; Gentemann et al., 2017). In this context, organic semiconductors allow to establish almost seamless abiotic/biotic interfaces, as they are soft materials that support both ionic and electronic transport, alike many biological molecules (Rivnay et al., 2014). The triggering mechanism leading to cell activity upon light absorption can be capacitive, faradaic, or thermal (Đerek et al., 2020; Manfredi et al., 2021; Martino et al., 2015).

An alternative approach still based on organic molecules exploits photochromic compounds that can be covalently bound (Gorostiza and Isacoff, 2008; Izquierdo-Serra et al., 2016; Leippe et al., 2017) to an ion channel or not-covalently (Fang et al., 2020; Zhang et al., 2014) to the plasma membrane. This approach is gaining increasing interest due to the stimulation efficiency, its versatility and the possibility of using two photon absorption that pushes the stimulation

wavelengths to the near infrared spectral region, improving tissue penetration (Magome et al., 2011; Riefolo et al., 2019).

In this work, we describe a new tool for optical pacing of human-induced pluripotent stem cell-derived CMs (hiPSC-CMs) exploiting Ziapin2, a recently synthetized intramembrane photochromic transducer that we successfully tested in bacteria, non-excitable cells and neurons (DiFrancesco et al., 2020; Giuseppe Maria Paternò et al., 2020; Giuseppe M. Paternò et al., 2020; Vurro et al., 2021; Magni et al., 2021).

Ziapin2 has affinity for the hiPSC-CMs sarcolemma and once partitioned, it undergoes photoisomerization, which in turn leads to the membrane capacitance modulation. In dark, cells treated by Ziapin2 show increased capacitance as the result of reduction in membrane thickness, slightly modifying the equilibrium condition without further effects. Upon millisecond pulses of visible light, *trans*→*cis* isomerization causes a fast drop of capacitance due to membrane relaxation, resulting in a transient hyperpolarization followed by a delayed depolarization that triggers AP generation. The increase in AP frequency nicely correlates with changes in Ca^{2+} dynamics and contraction rate, thus proving that Ziapin2 modulates excitation-contraction (E-C) coupling at a whole extent.

2. Results and Discussion

2.1. Ziapin2 photoisomerization modulates hiPSC-CMs membrane potential

The molecule was tested at two different concentrations (5 µM and 25 µM). In both cases once added to hiPSC-CMs cultures, Ziapin2 successfully partitioned into the sarcolemma causing a significant increase in capacitance (**Figure S1a**). The effect was concentration dependent, as we observed a +23% (14.2 ± 1.2 pF vs 17.5 ± 0.9 pF; $p = 0.05089$) for 5 µM and +56% (14.2 ± 1.2 pF vs 22.2 ± 1.3 pF; $p = 0.00063$) for 25 µM, while no alterations were detected in hiPSC-CMs incubated with the vehicle (DMSO, data not shown). At equilibrium, this phenomenon changes the membrane electrical time constant (RC) but not the resting potential. According to previous experimental evidences (DiFrancesco et al., 2020; Giuseppe Maria Paternò et al., 2020; Vurro et al., 2021), the modulation has been ascribed to the thinning of the bilayer caused by the dimerization of Ziapin2 molecules inside the membrane.

Upon photostimulation the azobenzene isomerization removes the geometric constraint of the dimer leading to membrane relaxation and a partial return towards steady-state capacitance values with a reduction of -14% (17.5 ± 0.9 pF vs 15.0 ± 0.7 pF; $p = 0.08$) and -12% (22.2 ± 1.3 pF vs 19.5 ± 1.1 pF; $p = 0.14$) for 5 and 25 µM Ziapin2, respectively (**Figure S1b**).

Whole-cell patch clamp experiments in current clamp mode revealed that the photo-induced drop in capacitance correlates with a modulation of the membrane potential. In particular, the Ziapin2-mediated photostimulation (with 20 and 200 ms single light pulses) results in a transient hyperpolarization that is occurring within few ms after the light onset, consistent with the linear inverse relation between capacitance and voltage. The recovery of the potential by capacitive currents is followed by a depolarization which is often large enough to generate an AP (see representative traces in **Figure 1a**).

Both hyperpolarization and depolarization peaks display much higher amplitude at 25 µM concentration than 5 µM (**Figure 1b**). For instance, with 20 ms light stimulation hyperpolarization is 6 times larger at 25 µM concentration, even if the relative change in capacitance is comparable (-14% vs -12% for 5 and 25µM Ziapin2, respectively, see **Figure S1b**). This is surprising, since according to the simple plane capacitor model, if there are no other changes in the circuit, $\Delta V/V=\Delta C/C$. To explain this discrepancy, we conjecture that equal amplitude, but faster changes in capacitance, could give rise to larger changes in membrane potential. This is confirmed by a numerical simulation based on the equivalent circuit model for the membrane (**Figure S2**). To account for the different kinetics, we propose that Ziapin2 at lower concentration preferentially dwells in the lipid drafts of the membrane, where isomerization is slower, while at higher concentration it can spread to other domains where isomerization occurs faster (DiFrancesco et al., 2020). In agreement with capacitance data, no light-dependent effects were noticed in vehicle-treated hiPSC-CMs (**Figure 1**).

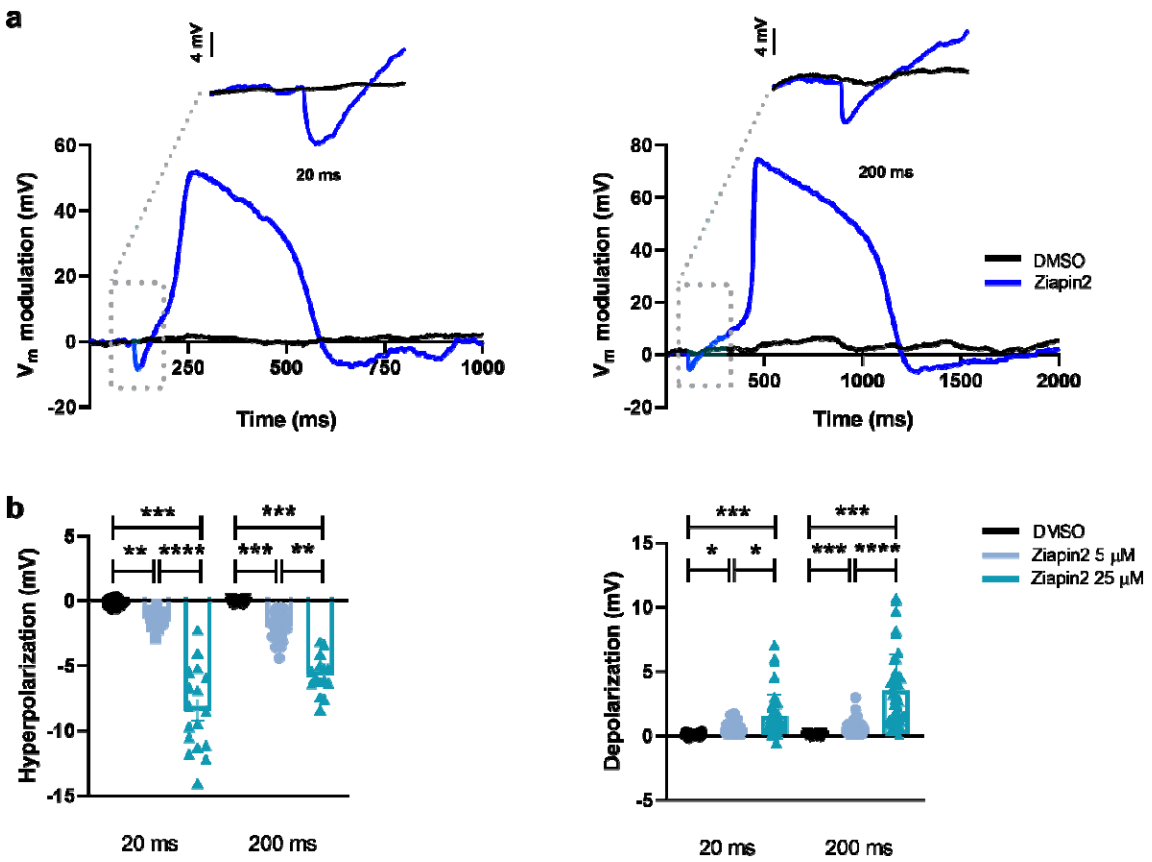

Figure 1. Ziapin2 mediates a light-evoked membrane voltage modulation in hiPSC-CMs. a) *Representative whole-cell current-clamp traces recorded in cells loaded with either vehicle (DMSO, in black) or Ziapin2 (blue) and stimulated with 20 ms- (left) or 200 ms-long (right) single light pulses. Photoexcitation is represented by the cyan shaded area. Light power density, 80 mW/mm^2. The membrane potential modulation can be appreciated at a faster time scale in the inset of each panel.* ***b)*** *Scatter plots of the peak hyperpolarization (left) and depolarization (right) changes in hiPSC-CMs exposed to Ziapin2 (5 µM in sky blue, 25 µM in teal) or DMSO for the above-mentioned light-stimulation protocols. n >18 for 5 µM and 25 µM Ziapin2 loaded cells and n = 20 for DMSO-treated hiPSC-CMs. V_m values have been reported as relative variation to better appreciate the light-induced effect; however, no significant changes were detected in the resting membrane potential values (Ziapin2 5µM Vm = -42.4 ± 3.9 mV; Ziapin2 25µM Vm = -42.8 ± 2.6 mV; DMSO Vm = -37 ± 4.4 mV). The experiments were carried out at room temperature (24°C). Data were collected from three independent differentiations and are represented as mean ± sem. * p < 0.05, ** p < 0.01, *** p < 0.001 and **** p < 0.0001.*

2.2. Ziapin2 photoisomerization induces AP firing in hiPSC-CMs

To assess the impact of the molecule on hiPSC-CMs electrical activity, we evaluated the ability of light stimulation to generate APs in hiPSC-CMs loaded with Ziapin2. Remarkably, the most striking effect was observed in CMs exposed to the highest photochromic concentration (72 ± 4% of responding cells for Ziapin2 25 µM vs 37 ± 3 % for Ziapin2 5 µM, **Figure 2a**).

As a next step, we compared spontaneous and light-evoked AP features. Since the most significant effects occurred in hiPSC-CMs loaded with Ziapin2 25 µM and subjected to 20 ms light stimuli, here we report only data within these experimental conditions.

In dark conditions no significant differences were measured in maximum diastolic potential (MDP, **Figure S3a**) and maximal upstroke velocity (dV/dt_{max}, **Figure S3b**), while AP amplitude (APA, **Figure S3c**) was slightly decreased in Ziapin2-exposed CMs (70.3 ± 1.2 mV vs 70.8 ± 2.9 mV; $p = 0.04$). Ziapin2 photoisomerization did not exert any detectable modification of these AP parameters (**Figure S3b and S3c**), while a light-triggered increase in the number of AP per unit time was observed (0.14 ± 0.02 Hz vs 0.27 ± 0.02 Hz for spontaneous and light-evoked respectively; $p < 0.0001$, **Figure 2b**). This light-induced frequency increment was associated with a shortening of the AP duration; plotting the standard deviation of these two parameters, it was possible to notice a greater clustering of both the indicators upon illumination (**Figure 2c)**. This result suggests that Ziapin2 can potentially play a pivotal role in regulating the asynchronous activity of cardiac cells and tissues by reducing the overall beating variabilities. Interestingly, a punctual AP generation was obtained stimulating the cells with a train of 20 ms light pulses at 0.5 Hz, observing just very few failures under rate-controlled conditions (**Figure 2d**).

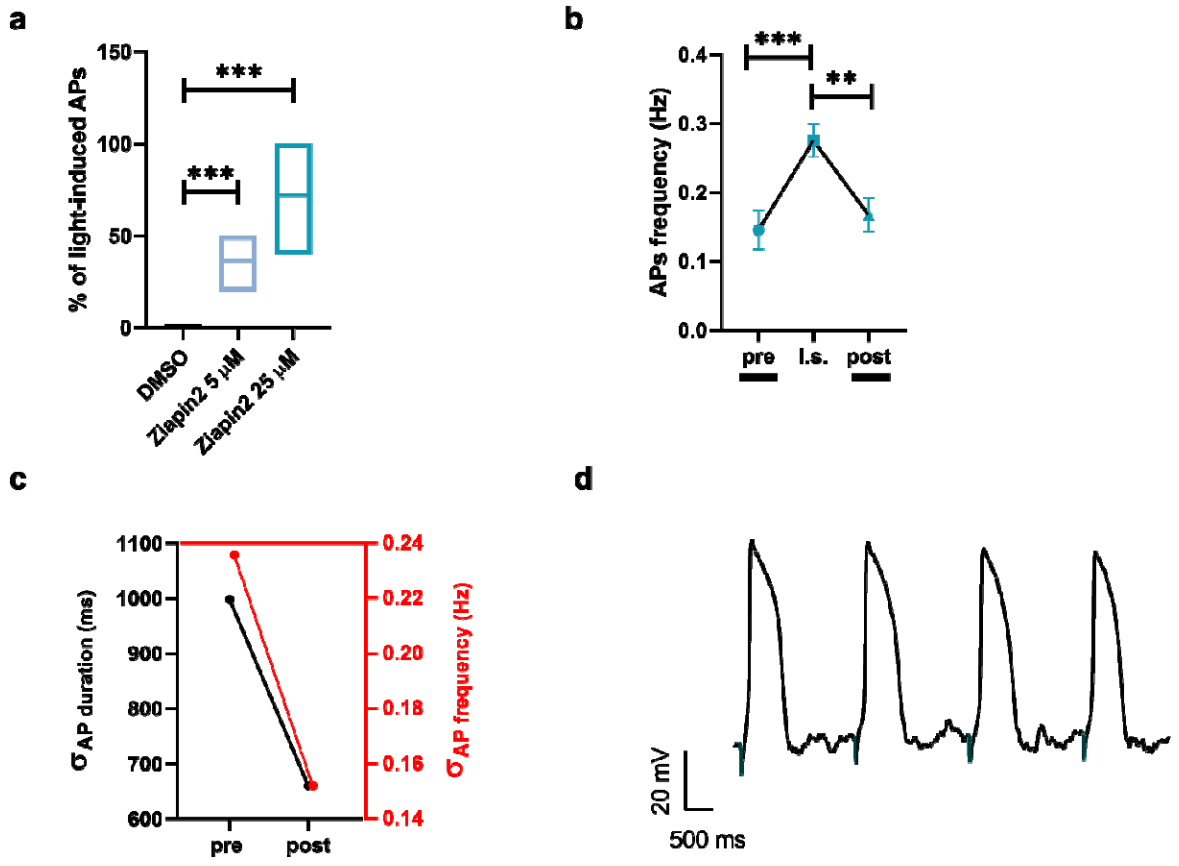

Figure 2. Light-evoked AP modulation by Ziapin2 in hiPSC-CMs. a) *Box plots (line at mean) of the reproducibility of the light-induced AP generation in cells loaded with either vehicle (DMSO, in black) or Ziapin2 (5 µM, in sky blue; 25 µM, in teal). The percentage represents the n° of AP directly generated by each light pulse.* ***b)*** *AP frequency before (pre), during (l.s.), and after (post) light stimulation. Data are represented as mean ± sem; n > 40 for each condition from three independent differentiations.* ***c)*** *Correlation between the standard deviation (σ) of AP duration (left, black) and frequency (right, red) pre- and post- photostimulation.* ***d)*** *Representative traces of APs generated in response to a light train stimulation (20 ms cycle length; 0.5 Hz stimulation frequency, represented as cyan shaded areas). Light power density, 80 mW/mm^2. The experiments were carried out at room temperature (24°C). ** p < 0.01 and *** p < 0.001.*

2.3. Ziapin2 photoisomerization alters Ca^{2+} dynamics in hiPSC-CMs

In CMs the AP triggers the E-C coupling, namely the physiological process that converts an electrical stimulus to a mechanical response. It is well established that the contraction of cardiac cells is triggered by a considerable increase in intracellular Ca^{2+} concentration. We thus evaluated Ziapin2 effect on cytoplasmic Ca^{2+} levels performing fluorescence-based measurements with the

widely used Ca^{2+} indicator Fluo-4 AM (Gee et al., 2000) (**Figure 3**). Based on the substantial overlap between Fluo-4 and Ziapin2 absorption and emission spectra (**Figure S4**), we used pulsed light stimulation (1 Hz, 50% duty cycle, 500 ms duration) both to trigger molecule photoisomerization and to excite the fluorophore. The protocol is fast enough to temporally resolve the Ca^{2+} transient (CaT, **Figure 3b**). Cells incubated with the fluorophore only were used as a negative control.

We observed that photostimulated Ziapin2-loaded cells presented +26.3% in the number of cells showing Ca^{2+} dynamics (in comparison to controls ($p = 0.007$ **Figure 3a**). Light induced CaTs displayed also an increased amplitude (F/F_0: 3.47 ± 0.18 vs 2.91 ± 0.26 vs, $p = 0.018$, **Figure 3c**), a slightly reduced duration (9.14 ± 0.24 s vs 10.16 ± 0.34 s, $p = 0.14$, **Figure 3d**) net of an augmented frequency (+35 %, $p = 0.0009$, **Figure 3e**). Notably, no differences were detected in the time to CaT peak (ttp) and half-time of CaT decay (decay $t_{1/2}$), thus suggesting that CaT morphology was not affected by Ziapin2 photoisomerization.

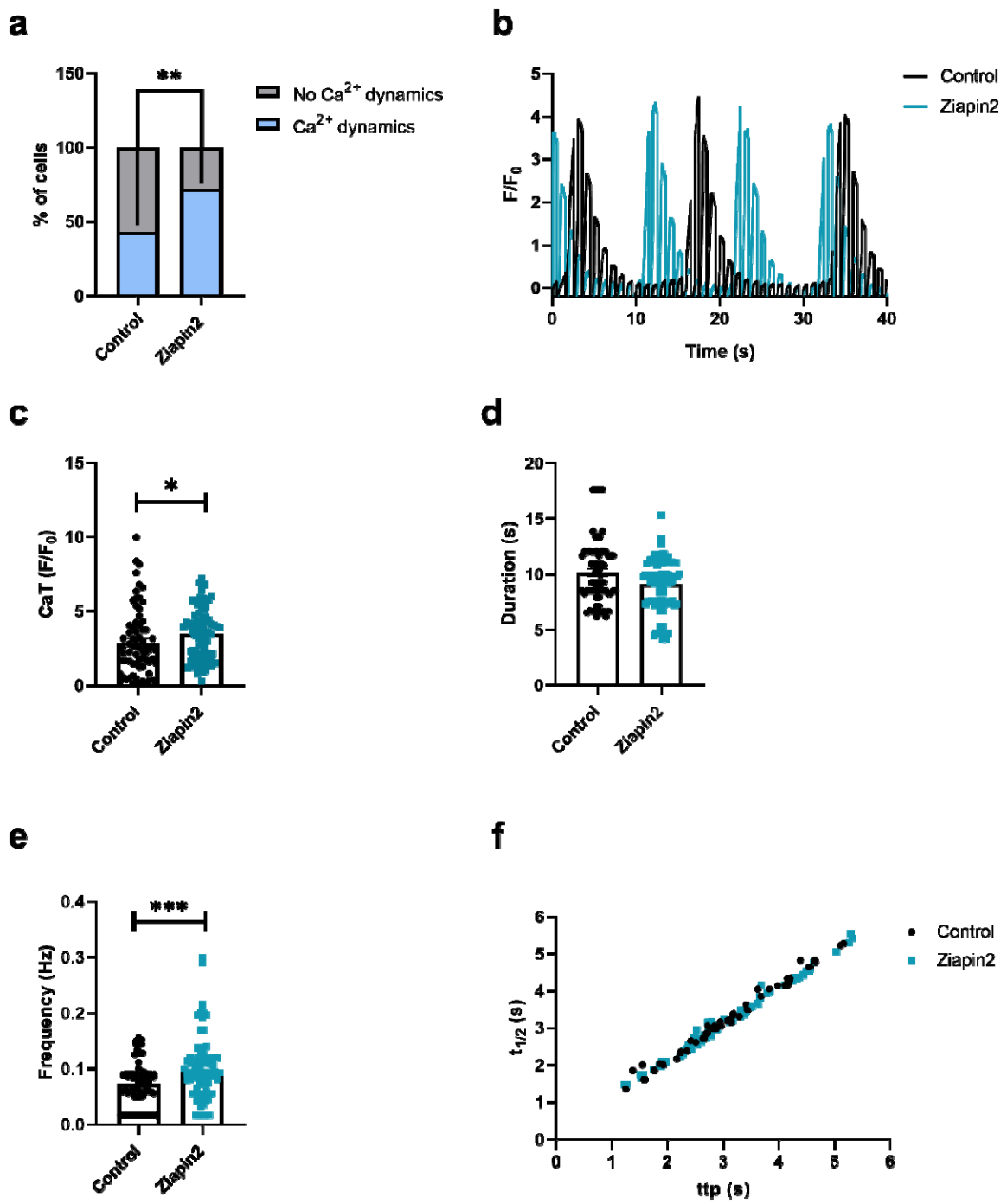

Figure 3. Photo-induced Calcium dynamics in Ziapin2-loaded hiPSC-CMs. a) *Ziapin2-mediated light stimulation increases the percentage of cells displaying Ca^{2+} dynamics (Control n = 72; Ziapin2 n = 89 from three independent differentiations).* ***b)*** *Representative Ca^{2+} transients (CaTs) acquired during a pulsed light stimulation (Ctrl in black and Ziapin2-treated cells in teal) at light power density = 5.8 mW/mm^2.* ***c)*** *CaT amplitude,* ***d)*** *Duration,* ***e)*** *Frequency, and* ***f)*** *Correlation between half time decay ($t_{1/2}$) and time to peak (ttp) in hiPSC-CMs treated with Ziapin2 25 μM*

*(teal) and relative controls (black). The experiments were carried out at room temperature (24°C). * $p < 0.05$, ** $p < 0.01$, and *** $p < 0.001$.*

2.4. Ziapin2 photoisomerization enhances hiPSC-CMs contraction rate

As a final step, we investigated the effect of Ziapin2 on hiPSC-CMs contraction behaviour by exploiting a custom MATLAB code to assess the contraction frequency from previously acquired high-speed movies of cells subjected to the same photostimulation protocol used for Ca^{2+} dynamics measurements.

In dark conditions, Ziapin2-loaded hiPSC-CMs had a contraction rate of 0.19 ± 0.01 Hz. Under 1 Hz pulsed illumination the rate increased by 35% during the entire acquisition window. The effect persisted in the 30 seconds following light offset, albeit with a 12% decrease (from 0.26 ± 0.01 Hz to 0.23 ± 0.01 Hz, **Figure 4a**). The persistent higher contraction frequency is probably ascribed to our experimental conditions. First, the experiments were performed at 24°C, a temperature far from the canonical physiological 37°C that could have slowed down the cell behavior (Francesco Lodola et al., 2019). Secondly, even though the hiPSC-CMs are a consolidated tool and hold an enormous potential in cardiovascular research, their E-C coupling process resembles more the one of fetal/neonatal CMs, thus it is possible that the Ca^{2+} clearance machinery in these cells is substantially slower in comparison to adult CMs (Kane et al., 2015; Lodola et al., 2021). Conversely, no differences were detected in vehicle treated hiPSC-CMs subjected to the same stimulation protocol (**Figure S5**). Remarkably, the lower the spontaneous hiPSC-CMs contraction rate, the higher the light induced frequency increase.

To better characterize the involvement of Ziapin2 in the light-induced increase in contraction frequency, we measured the latency, calculated as the interval between the onset of stimulation and the contraction of the CMs (**Figure 4b**). The timescale was found to be distributed around 500 ms in a non-stochastic way, compatibly, at least in these experimental conditions, with expected times for the electromechanical coupling, thus confirming the link between optical stimulus and increased contraction.

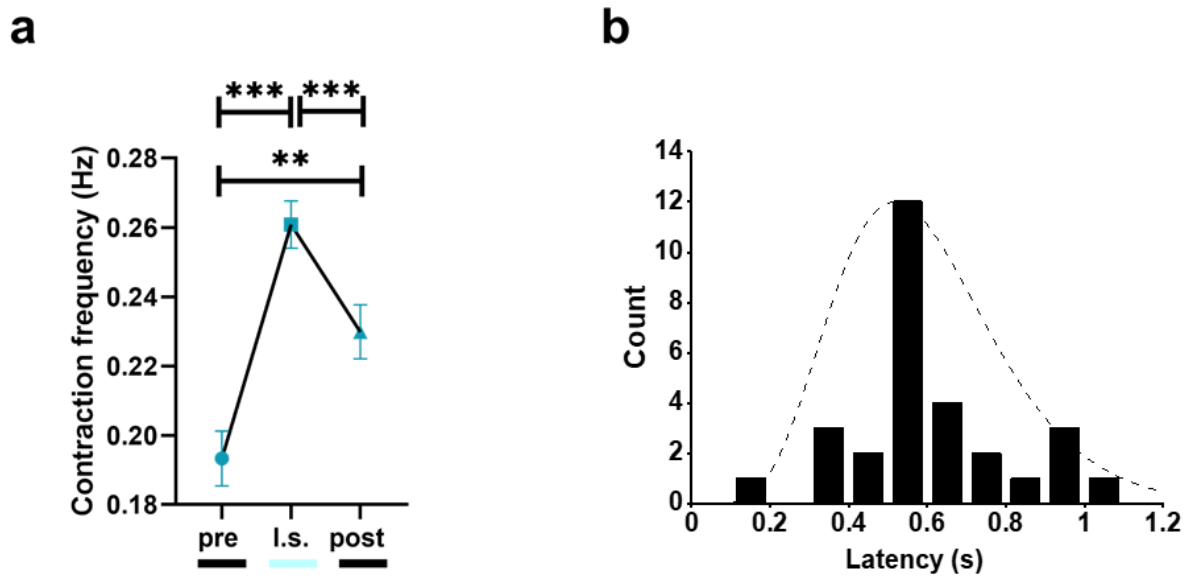

Figure 4. Light-induced contraction rate modulation in Ziapin2 loaded hiPSC-CMs. a) *Ziapin2-treated hiPSC-CMs contraction frequency before (pre), during (l.s.), and after (post) 1 Hz pulsed light stimulation at light power density = 30 mW/mm^2 (n = 346 from three independent differentiations, data are shown as mean ± sem).* ***b)*** *Time to contraction measured from the light onset in quiescent hiPSC-CMs (n = 30). The cell response time distribution peaks at 500 ms, highlighting a correlation between light stimulation and cell's functional response. A gamma function has been used as a guide to the eye of this time distribution. The experiments were carried out at room temperature (24°C). ** $p < 0.01$ and *** $p < 0.001$.*

3. Conclusions & Perspectives

The possibility to manipulate the cellular activity with a precise spatial and temporal punctuality is a key enabling technology for biology and medicine. In this work we report the first proof-of-principle demonstration of Ziapin2 as a light-sensitive tool to control cardiac cell excitability and contractility. Our approach is innovative for a series of reasons: i) unlike electrical stimulation, it enables a non-contact and reversible excitation with high spatio-temporal precision; ii) it avoids genetic manipulation and the pitfalls related to the introduction of exogenous genetic material using viral vectors, thus overcoming the major drawback of optogenetics; iii) Ziapin2 primarily targets the cellular passive properties without affecting ionic conductances, an issue shared by both optogenetics and photoswitchable ligands, still allowing a millisecond control of V_m; iv) the molecule effect is heatless, thus preventing increases in temperature that could be potentially harmful to the cells over the long term.

Ziapin2 could be used as a non-invasive optical tool to control cardiac electrical activity for bio-hybrid robotics studies (in which CMs are often the biological substrate), thus enabling or simplifying design and fabrication of the actuators (Park et al., 2016; Raman et al., 2016; Vurro et al., 2022). Also, the possibility to pattern light in cardiac organoids or microtissues will allow to address fundamental questions of cardiac biology.

4. Limitations of the study

Further studies are needed to allow the elucidation of biophysical mechanisms ruling the photo-stimulation process, focusing in particular on the triggering mechanism that leads to AP generation. Moreover, some chemical improvement should be faced to increase the molecular absorption cross section leading to a reducing of the required light power density. Similarly, to further corroborate our findings, we will extend this approach to fully differentiated, adult cardiomyocytes. This will be an important step to show that our molecules do work in a more complex and physiological scenario.

If successful, this would open a broader field of applications for light-mediated clinical treatment of cardiac arrhythmias. In this context, new curative strategies that are less invasive, long-lasting, and less power consuming than the existing ones are a *conditio sine qua non* to reduce the burden for the recipients.

4. Materials and Methods

Synthesis and characterization of Ziapin2

Ziapin2 was synthetized as previously described (DiFrancesco et al., 2020; Giuseppe Maria Paternò et al., 2020; Vurro et al., 2021).

hiPSC-CMs preparation

Two different batches of hiPSC-CMs were used for this study, a commercial one (Pluricyte® CMs provided by Ncardia, Gosselies, Belgium) and a laboratory handle one. The latter was produced by directed cardiac differentiation of previously generated control hiPSCs (Di Pasquale et al., 2013; Francesco Lodola et al., 2019; Lodola et al., 2016).

In brief, cardiac induction and generation of hiPSC-CMs were obtained as previously reported, using a chemically-defined serum-free protocol, which is based on activation (CHIR99021) and inhibition (IWR1) of the Wnt pathway in RPMI-B27 medium (Lian et al., 2013; Nakahama and Di Pasquale, 2016; Salvarani et al., 2019). In this work, CMs were differentiated from two different control iPSC lines (one male and one female) between the 18th and the 35th passage in culture. Importantly, employed cell lines were regularly tested for being free of major chromosomal abnormalities by karyotype analysis. CMs were used for the experiments 25–30 days after spontaneous contracting activity was started, a differentiation stage at which they expressed the repertoire of sarcomeric proteins, calcium regulators, and ionic channels necessary for their correct functionality. The commercial batch was thawed and cultured following the manufacturer's protocol. In terms of plating density, cells for both batches were seeded onto the material at a confluence comprised between 50% and 60% on fibronectin coated (15 μg/ml in PBS buffer solution) 18-mm round glass coverslip (VWR, Radnor, USA). The cells were maintained in incubator at 37°C and 5% CO_2.

Electrophysiology

Standard whole-cell patch clamp recordings were performed on isolated cells with an Axopatch 200B (Axon Instruments) coupled with a Nikon Eclipse Ti inverted microscope. Acquisitions were performed with freshly pulled glass pipettes (4-7 MΩ), filled with the following intracellular solution [mM]: 12 KCl, 125 K-Gluconate, 1 MgCl2, 0.1 CaCl2, 10 EGTA, 10 HEPES, 10 ATP-Na2. The extracellular solution contained [mM]: 135 NaCl, 5.4 KCl, 5 HEPES, 10 Glucose, 1.8 CaCl2, 1 MgCl2. Acquisitions were performed with pClamp-10 software (Axon Instruments). Membrane currents were low pass filtered at 2 kHz and digitized with a sampling rate of 10 kHz (Digidata 1440 A, Molecular Devices).

A cyan excitation light (λ_{ex} = 470 nm) was provided by a LED system (Lumencor Spectra X) coupled to the fluorescence port of the microscope through a liquid-fibre. The photoexcitation density was 80 mW/mm^2, as measured at the output of the 40X microscope objective (Pobj). Hyperpolarization and depolarization were measured as the minimum and maximum voltage, respectively, reached within 350 ms from the light-onset. Data were analyzed with Origin 9.0 (OriginLab Corporation) and MATLAB (MathWorks).

Capacitance recordings

Capacitance measurements were performed as previously described (Vurro et al., 2020, 2021). Briefly, a double sinusoidal voltage-clamp signal was applied to the cell in whole-cell configuration. The response current signal was acquired, and membrane capacitance and resistance were extracted fitting the current with a custom MATLAB program. The capacitance value was extracted in dark condition and during light stimulation (20 ms pulse). The shorter pulse was used in order to take into account mainly the effect related to Ziapin2 photoisomerization.

Intracellular Ca^{2+} measurements

Intracellular Ca^{2+} measurements were performed with an upright Olympus microscope and the extracellular solution was the one used for the electrophysiology measurements. Ca^{2+} dynamic was recorded in spontaneous beating hiPSC-CMs incubated with 2.5 µM Fluo-4 AM probe (Ex/Em 470/515 nm) for 20 minutes and washed out for 10 minutes with extracellular solution. Ziapin2 and Fluo-4 AM excitations were provided by the same blue LED light source (474 nm, Lumencor Spectra III), at power density of 5.8 mW/mm^2. This value was used in order to avoid Fluo-4 AM possible bleaching. ImageJ program was used for the analysis of the fluorescent signal, a region of interest (ROI) corresponding to one cell. Fluorescent values (F) were normalizer to F value (F_0) recorded at the beginning of the protocol. The following parameters were evaluated for Ca^{2+} dynamic recording: CaT amplitude (CaT peak – baseline value), CaT duration (as duration from start to end of CaT events); time to CaT peak (ttp), half-time of CaT decay ($t_{1/2}$) and spontaneous beating frequency.

Acquisition and analysis of hiPSC-CMs contractile behaviour

The microscope described before was used to stimulate (Lumencor Spectra X, λ_{ex} = 470 nm, 20X objective, Pobj = 30 mW/mm^2) and acquire video of the CMs contraction a frequency. An objective with a lower magnification was used in order to increase the amount of recorder cells resulting in a more robust analisys. Consequently, the resulting power density was lower due to the bigger area.

Contractile behavior was analyzed using a custom-built algorithm, implemented in MATLAB R2020a. The approach is based on the contraction-induced retraction of cell body towards nucleus and is effective even if there is no displacement of cell extremities or if the cellular edge cannot be detected properly.

Basically, for each CM a set of features belonging to the cell body is identified and tracked across video frames by means of Kanade-Lucas-Tomasi algorithm (Jianbo Shi and Tomasi, 1994; Lucas and Kanade, n.d.). Averaging the estimated motion fields of all these feature points returns a mean geometric transformation, which can be applied to a bounding box delimiting the region of interest. The area of this bounding box is measured over time and presents minima at cellular contractions. The number of contractions per time interval yields an estimate of the cell contraction rate. Data were analyzed with Origin 9.0 (OriginLab Corporation).

Statistical analysis

Data were expressed as means ± sem. Normal distribution was assessed using D'Agostino-Pearson's normality test. To compare two sample groups, either the Student's t-test or the Mann-Whitney U-test was used. To compare more than two sample groups, one-way ANOVA or Kruskal-Wallis were used. $p < 0.05$ was considered statistically significant. The analysis was carried out using OriginPro-8 (OriginLab) and Prism (GraphPad software, Inc.,La Jolla, CA).

Acknowledgements

This research was supported by: Fondo di Ateneo (2020-ATE-0044) from the University of Milano-Bicocca (F.L.), Nanosparks project (ID 2018–0505) from Fondazione Cariplo (G.L.), EU Horizon 2020 FETOPEN-2018-2020 Programme 'LION-HEARTED', grant agreement n. 828984 (M.R.A., F.L., C.R., E.D.P.), European Research Council (ERC) under the European Union's Horizon 2020 research and innovation program 'LINCE', grant agreement n. 803621 (M.R.A.).

Graphical Abstract created with BioRender.com.

Author contributions

Vito Vurro: Conceptualization, Data curation, Formal analysis, Investigation, Writing – review & editing; Beatrice Federici: Data curation, Formal analysis, Investigation; Carlotta Ronchi**:** Data curation, Formal analysis, Investigation; Valentina Sesti**:** Investigation, Methodology; Silvia Crasto**:** Investigation, Methodology; Claudia Maniezzi**:** Data curation, Formal analysis; Maria Rosa Antognazza**:** Investigation, Methodology, Supervision; Chiara Bertarelli**:** Investigation, Methodology, Supervision; Elisa Di Pasquale**:** Investigation, Methodology, Supervision; Guglielmo

Lanzani**:** Conceptualization, Funding acquisition, Investigation, Resources, Supervision, Validation, Writing –review & editing; Francesco Lodola**:** Conceptualization, Funding acquisition, Investigation, Project administration, Supervision,Validation, Writing – original draft.

Declaration of Competing Interest

Declarations of interests: none.

References

Ambrosi, C.M., Klimas, A., Yu, J., Entcheva, E., 2014. Cardiac applications of optogenetics. Progress in Biophysics and Molecular Biology 115, 294–304. https://doi.org/10.1016/j.pbiomolbio.2014.07.001

Antognazza, M.R., Martino, N., Ghezzi, D., Feyen, P., Colombo, E., Endeman, D., Benfenati, F., Lanzani, G., 2015. Shedding Light on Living Cells. Adv. Mater. 27, 7662–7669. https://doi.org/10.1002/adma.201403513

Asano, T., Igarashi, H., Ishizuka, T., Yawo, H., 2018. Organelle Optogenetics: Direct Manipulation of Intracellular Ca2+ Dynamics by Light. Front. Neurosci. 12, 561. https://doi.org/10.3389/fnins.2018.00561

Bareket-Keren, L., Hanein, Y., 2014. Novel interfaces for light directed neuronal stimulation: advances and challenges. IJN 65. https://doi.org/10.2147/IJN.S51193

Biasci, V., Santini, L., Marchal, G.A., Hussaini, S., Ferrantini, C., Coppini, R., Loew, L.M., Luther, S., Campione, M., Poggesi, C., Pavone, F.S., Cerbai, E., Bub, G., Sacconi, L., 2022. Optogenetic manipulation of cardiac electrical dynamics using sub-threshold illumination: dissecting the role of cardiac alternans in terminating rapid rhythms. Basic Res Cardiol 117, 25. https://doi.org/10.1007/s00395-022-00933-8

Boyle, P.M., Karathanos, T.V., Trayanova, N.A., 2018. Cardiac Optogenetics: 2018. JACC: Clinical Electrophysiology 4, 155–167. https://doi.org/10.1016/j.jacep.2017.12.006

Bruegmann, T., Malan, D., Hesse, M., Beiert, T., Fuegemann, C.J., Fleischmann, B.K., Sasse, P., 2010. Optogenetic control of heart muscle in vitro and in vivo. Nat Methods 7, 897–900. https://doi.org/10.1038/nmeth.1512

Bruno, G., Melle, G., Barbaglia, A., Iachetta, G., Melikov, R., Perrone, M., Dipalo, M., De Angelis, F., 2021. All-Optical and Label-Free Stimulation of Action Potentials in Neurons and Cardiomyocytes by Plasmonic Porous Metamaterials. Adv. Sci. 2100627. https://doi.org/10.1002/advs.202100627

Crocini, C., Ferrantini, C., Coppini, R., Scardigli, M., Yan, P., Loew, L.M., Smith, G., Cerbai, E., Poggesi, C., Pavone, F.S., Sacconi, L., 2016. Optogenetics design of mechanistically-based stimulation patterns for cardiac defibrillation. Sci Rep 6, 35628. https://doi.org/10.1038/srep35628

Deisseroth, K., 2015. Optogenetics: 10 years of microbial opsins in neuroscience. Nat Neurosci 18, 1213–1225. https://doi.org/10.1038/nn.4091

Deisseroth, K., 2011. Optogenetics. Nat Methods 8, 26–29. https://doi.org/10.1038/nmeth.f.324

Đerek, V., Rand, D., Migliaccio, L., Hanein, Y., Głowacki, E.D., 2020. Untangling Photofaradaic and Photocapacitive Effects in Organic Optoelectronic Stimulation Devices. Front. Bioeng. Biotechnol. 8, 284. https://doi.org/10.3389/fbioe.2020.00284

Di Maria, F., Lodola, F., Zucchetti, E., Benfenati, F., Lanzani, G., 2018. The evolution of artificial light actuators in living systems: from planar to nanostructured interfaces. Chem. Soc. Rev. 47, 4757–4780. https://doi.org/10.1039/C7CS00860K

Di Pasquale, E., Lodola, F., Miragoli, M., Denegri, M., Avelino-Cruz, J.E., Buonocore, M., Nakahama, H., Portararo, P., Bloise, R., Napolitano, C., Condorelli, G., Priori, S.G., 2013. CaMKII inhibition rectifies arrhythmic phenotype in a patient-specific model of catecholaminergic polymorphic ventricular tachycardia. Cell Death Dis 4, e843–e843. https://doi.org/10.1038/cddis.2013.369

DiFrancesco, M.L., Lodola, F., Colombo, E., Maragliano, L., Bramini, M., Paternò, G.M., Baldelli, P., Serra, M.D., Lunelli, L., Marchioretto, M., Grasselli, G., Cimò, S., Colella, L., Fazzi, D., Ortica, F., Vurro, V., Eleftheriou, C.G., Shmal, D., Maya-Vetencourt, J.F., Bertarelli, C., Lanzani, G., Benfenati, F., 2020. Neuronal firing modulation by a membrane-targeted photoswitch. Nat. Nanotechnol. 15, 296–306. https://doi.org/10.1038/s41565-019-0632-6

Duebel, J., Marazova, K., Sahel, J.-A., 2015. Optogenetics: Current Opinion in Ophthalmology 26, 226–232. https://doi.org/10.1097/ICU.0000000000000140

Dwenger, M., Kowalski, W.J., Ye, F., Yuan, F., Tinney, J.P., Setozaki, S., Nakane, T., Masumoto, H., Campbell, P., Guido, W., Keller, B.B., 2019. Chronic optical pacing conditioning of h-iPSC engineered cardiac tissues. J Tissue Eng 10, 204173141984174. https://doi.org/10.1177/2041731419841748

Fang, J., Liu, D., Xu, D., Wu, Q., Li, H., Li, Y., Hu, N., 2022. Integrated Au-Nanoroded Biosensing and Regulating Platform for Photothermal Therapy of Bradyarrhythmia. Research 2022, 1–14. https://doi.org/10.34133/2022/9854342

Fang, Y., Meng, L., Prominski, A., Schaumann, E.N., Seebald, M., Tian, B., 2020. Recent advances in bioelectronics chemistry. Chem. Soc. Rev. 10.1039.D0CS00333F. https://doi.org/10.1039/D0CS00333F

Feiner, R., Dvir, T., 2019. A ray of light for treating cardiac conduction disorders. Proc Natl Acad Sci USA 116, 347–349. https://doi.org/10.1073/pnas.1819948116

Fenno, L., Yizhar, O., Deisseroth, K., 2011. The Development and Application of Optogenetics. Annu. Rev. Neurosci. 34, 389–412. https://doi.org/10.1146/annurev-neuro-061010-113817

Ferenczi, E.A., Tan, X., Huang, C.L.-H., 2019. Principles of Optogenetic Methods and Their Application to Cardiac Experimental Systems. Front. Physiol. 10, 1096. https://doi.org/10.3389/fphys.2019.01096

Floria, M., Radu, S., Gosav, E.M., Moraru, A.C., Serban, T., Carauleanu, A., Costea, C.F., Ouatu, A., Ciocoiu, M., Tanase, D.M., 2020. Cardiac Optogenetics in Atrial Fibrillation: Current Challenges and Future Opportunities. BioMed Research International 2020, 1–13. https://doi.org/10.1155/2020/8814092

Gee, K.R., Brown, K.A., Chen, W.-N.U., Bishop-Stewart, J., Gray, D., Johnson, I., 2000. Chemical and physiological characterization of fluo-4 Ca2+-indicator dyes. Cell Calcium 27, 97–106. https://doi.org/10.1054/ceca.1999.0095

Gentemann, L., Kalies, S., Coffee, M., Meyer, H., Ripken, T., Heisterkamp, A., Zweigerdt, R., Heinemann, D., 2017. Modulation of cardiomyocyte activity using pulsed laser irradiated gold nanoparticles. Biomed. Opt. Express 8, 177. https://doi.org/10.1364/BOE.8.000177

Gorostiza, P., Isacoff, E.Y., 2008. Optical Switches for Remote and Noninvasive Control of Cell Signaling. Science 322, 395–399. https://doi.org/10.1126/science.1166022

Hopkins, J., Travaglini, L., Lauto, A., Cramer, T., Fraboni, B., Seidel, J., Mawad, D., 2019. Photoactive Organic Substrates for Cell Stimulation: Progress and Perspectives. Adv. Mater. Technol. 4, 1800744. https://doi.org/10.1002/admt.201800744

Huang, C.L.-H., Ferenczi, E.A., Lei, M., 2020. Editorial: Optogenetics: An Emerging Approach in Cardiac Electrophysiology. Front. Physiol. 11, 414. https://doi.org/10.3389/fphys.2020.00414

Izquierdo-Serra, M., Bautista-Barrufet, A., Trapero, A., Garrido-Charles, A., Díaz-Tahoces, A., Camarero, N., Pittolo, S., Valbuena, S., Pérez-Jiménez, A., Gay, M., García-Moll, A., Rodríguez-Escrich, C., Lerma, J., de la Villa, P., Fernández, E., Pericàs, M.À., Llebaria, A., Gorostiza, P., 2016. Optical control of endogenous receptors and cellular excitability using targeted covalent photoswitches. Nat Commun 7, 12221. https://doi.org/10.1038/ncomms12221

Jianbo Shi, Tomasi, 1994. Good features to track, in: Proceedings of IEEE Conference on Computer Vision and Pattern Recognition CVPR-94. Presented at the Proceedings of IEEE Conference on Computer Vision and Pattern Recognition, IEEE Comput. Soc. Press, Seattle, WA, USA, pp. 593–600. https://doi.org/10.1109/CVPR.1994.323794

Kane, C., Couch, L., Terracciano, C.M.N., 2015. Excitation–contraction coupling of human induced pluripotent stem cell-derived cardiomyocytes. Front. Cell Dev. Biol. 3. https://doi.org/10.3389/fcell.2015.00059

Knollmann, B.C., 2010. Pacing lightly: optogenetics gets to the heart. Nat Methods 7, 889–891. https://doi.org/10.1038/nmeth1110-889

Krueger, D., Izquierdo, E., Viswanathan, R., Hartmann, J., Pallares Cartes, C., De Renzis, S., 2019. Principles and applications of optogenetics in developmental biology. Development 146, dev175067. https://doi.org/10.1242/dev.175067

Leippe, P., Koehler Leman, J., Trauner, D., 2017. Specificity and Speed: Tethered Photopharmacology. Biochemistry 56, 5214–5220. https://doi.org/10.1021/acs.biochem.7b00687

Li, J., Li, H., Rao, P., Luo, J., Wang, X., Wang, L., 2021. Shining light on cardiac electrophysiology: From detection to intervention, from basic research to translational applications. Life Sciences 274, 119357. https://doi.org/10.1016/j.lfs.2021.119357

Lian, X., Zhang, J., Azarin, S.M., Zhu, K., Hazeltine, L.B., Bao, X., Hsiao, C., Kamp, T.J., Palecek, S.P., 2013. Directed cardiomyocyte differentiation from human pluripotent stem cells by modulating Wnt/β-

catenin signaling under fully defined conditions. Nat Protoc 8, 162–175. https://doi.org/10.1038/nprot.2012.150

Lodola, F., De Giusti, V.C., Maniezzi, C., Martone, D., Stadiotti, I., Sommariva, E., Maione, A.S., 2021. Modeling Cardiomyopathies in a Dish: State-of-the-Art and Novel Perspectives on hiPSC-Derived Cardiomyocytes Maturation. Biology 10, 730. https://doi.org/10.3390/biology10080730

Lodola, F., Morone, D., Denegri, M., Bongianino, R., Nakahama, H., Rutigliano, L., Gosetti, R., Rizzo, G., Vollero, A., Buonocore, M., Napolitano, C., Condorelli, G., Priori, S.G., Di Pasquale, E., 2016. Adeno-associated virus-mediated CASQ2 delivery rescues phenotypic alterations in a patient-specific model of recessive catecholaminergic polymorphic ventricular tachycardia. Cell Death Dis 7, e2393–e2393. https://doi.org/10.1038/cddis.2016.304

Lodola, F, Rosti, V., Tullii, G., Desii, A., Tapella, L., Catarsi, P., Lim, D., Moccia, F., Antognazza, M.R., 2019. Conjugated polymers optically regulate the fate of endothelial colony-forming cells. Science Advances 12.

Lodola, Francesco, Vurro, V., Crasto, S., Di Pasquale, E., Lanzani, G., 2019. Optical Pacing of Human-Induced Pluripotent Stem Cell-Derived Cardiomyocytes Mediated by a Conjugated Polymer Interface. Adv. Healthcare Mater. 8, 1900198. https://doi.org/10.1002/adhm.201900198

Lucas, B.D., Kanade, T., n.d. An Iterative Image Registration Technique with an Application to Stereo Vision 11.

Magni, A., Bondelli, G., Paternò, G.M., Sardar, S., Sesti, V., 2021. Azobenzene photoisomerization probes cell membrane nanoviscosity. arXiv 22. https://doi.org/arXiv:2107.03205

Magome, N., Kanaporis, G., Moisan, N., Tanaka, K., Agladze, K., 2011. Photo-Control of Excitation Waves in Cardiomyocyte Tissue Culture. Tissue Engineering Part A 17, 2703–2711. https://doi.org/10.1089/ten.tea.2010.0745

Manfredi, G., Lodola, F., Paternó, G.M., Vurro, V., Baldelli, P., Benfenati, F., Lanzani, G., 2021. The physics of plasma membrane photostimulation. APL Materials 9, 030901. https://doi.org/10.1063/5.0037109

Martino, N., Feyen, P., Porro, M., Bossio, C., Zucchetti, E., Ghezzi, D., Benfenati, F., Lanzani, G., Antognazza, M.R., 2015. Photothermal cellular stimulation in functional bio-polymer interfaces. Sci Rep 5, 8911. https://doi.org/10.1038/srep08911

Nakahama, H., Di Pasquale, E., 2016. Generation of Cardiomyocytes from Pluripotent Stem Cells. Methods Mol Biol 1353, 181–190. https://doi.org/10.1007/7651_2014_173

Negri, S., Faris, P., Tullii, G., Vismara, M., Pellegata, A.F., Lodola, F., Guidetti, G., Rosti, V., Antognazza, M.R., Moccia, F., 2022. Conjugated polymers mediate intracellular Ca2+ signals in circulating endothelial colony forming cells through the reactive oxygen species-dependent activation of Transient Receptor Potential Vanilloid 1 (TRPV1). Cell Calcium 101, 102502. https://doi.org/10.1016/j.ceca.2021.102502

Parameswaran, R., Koehler, K., Rotenberg, M.Y., Burke, M.J., Kim, J., Jeong, K.-Y., Hissa, B., Paul, M.D., Moreno, K., Sarma, N., Hayes, T., Sudzilovsky, E., Park, H.-G., Tian, B., 2019. Optical stimulation of cardiac cells with a polymer-supported silicon nanowire matrix. Proc Natl Acad Sci USA 116, 413–421. https://doi.org/10.1073/pnas.1816428115

Park, S.-J., Gazzola, M., Park, K.S., Park, S., Di Santo, V., Blevins, E.L., Lind, J.U., Campbell, P.H., Dauth, S., Capulli, A.K., Pasqualini, F.S., Ahn, S., Cho, A., Yuan, H., Maoz, B.M., Vijaykumar, R., Choi, J.-W., Deisseroth, K., Lauder, G.V., Mahadevan, L., Parker, K.K., 2016. Phototactic guidance of a tissue-engineered soft-robotic ray. Science 353, 158–162. https://doi.org/10.1126/science.aaf4292

Paternò, Giuseppe M., Bondelli, G., Sakai, V.G., Sesti, V., Bertarelli, C., Lanzani, G., 2020. The Effect of an Intramembrane Light-Actuator on the Dynamics of Phospholipids in Model Membranes and Intact Cells. Langmuir 36, 11517–11527. https://doi.org/10.1021/acs.langmuir.0c01846

Paternò, Giuseppe Maria, Colombo, E., Vurro, V., Lodola, F., Cimò, S., Sesti, V., Molotokaite, E., Bramini, M., Ganzer, L., Fazzi, D., D'Andrea, C., Benfenati, F., Bertarelli, C., Lanzani, G., 2020. Membrane Environment Enables Ultrafast Isomerization of Amphiphilic Azobenzene. Adv. Sci. 7, 1903241. https://doi.org/10.1002/advs.201903241

Raman, R., Cvetkovic, C., Uzel, S.G.M., Platt, R.J., Sengupta, P., Kamm, R.D., Bashir, R., 2016. Optogenetic skeletal muscle-powered adaptive biological machines. Proc Natl Acad Sci USA 113, 3497–3502. https://doi.org/10.1073/pnas.1516139113

Rand, D., Jakešová, M., Lubin, G., Vėbraitė, I., David-Pur, M., Đerek, V., Cramer, T., Sariciftci, N.S., Hanein, Y., Głowacki, E.D., 2018. Direct Electrical Neurostimulation with Organic Pigment Photocapacitors. Adv. Mater. 30, 1707292. https://doi.org/10.1002/adma.201707292

Rein, M.L., Deussing, J.M., 2012. The optogenetic (r)evolution. Mol Genet Genomics 287, 95–109. https://doi.org/10.1007/s00438-011-0663-7

Riefolo, F., Matera, C., Garrido-Charles, A., Gomila, A.M.J., Sortino, R., Agnetta, L., Claro, E., Masgrau, R., Holzgrabe, U., Batlle, M., Decker, M., Guasch, E., Gorostiza, P., 2019. Optical Control of Cardiac Function with a Photoswitchable Muscarinic Agonist. J. Am. Chem. Soc. 141, 7628–7636. https://doi.org/10.1021/jacs.9b03505

Rivnay, J., Owens, R.M., Malliaras, G.G., 2014. The Rise of Organic Bioelectronics. Chem. Mater. 26, 679–685. https://doi.org/10.1021/cm4022003

Salvarani, N., Crasto, S., Miragoli, M., Bertero, A., Paulis, M., Kunderfranco, P., Serio, S., Forni, A., Lucarelli, C., Dal Ferro, M., Larcher, V., Sinagra, G., Vezzoni, P., Murry, C.E., Faggian, G., Condorelli, G., Di Pasquale, E., 2019. The K219T-Lamin mutation induces conduction defects through epigenetic inhibition of SCN5A in human cardiac laminopathy. Nat Commun 10, 2267. https://doi.org/10.1038/s41467-019-09929-w

Sasse, P., Funken, M., Beiert, T., Bruegmann, T., 2019. Optogenetic Termination of Cardiac Arrhythmia: Mechanistic Enlightenment and Therapeutic Application? Front. Physiol. 10, 675. https://doi.org/10.3389/fphys.2019.00675

Savchenko, A., Cherkas, V., Liu, C., Braun, G.B., Kleschevnikov, A., Miller, Y.I., Molokanova, E., 2018. Graphene biointerfaces for optical stimulation of cells. Sci. Adv. 4, eaat0351. https://doi.org/10.1126/sciadv.aat0351

Starovoytov, A., Choi, J., Seung, H.S., 2005. Light-Directed Electrical Stimulation of Neurons Cultured on Silicon Wafers. Journal of Neurophysiology 93, 1090–1098. https://doi.org/10.1152/jn.00836.2004

Vurro, V., Bondelli, G., Sesti, V., Lodola, F., Paternò, G.M., Lanzani, G., Bertarelli, C., 2021. Molecular Design of Amphiphilic Plasma Membrane-Targeted Azobenzenes for Nongenetic Optical Stimulation. Frontiers in Materials 7, 10.

Vurro, V., Scaccabarozzi, A.D., Lodola, F., Storti, F., Marangi, F., Ross, A.M., Paternò, G.M., Scotognella, F., Criante, L., Caironi, M., Lanzani, G., 2020. A Polymer Blend Substrate for Skeletal Muscle Cells Alignment and Photostimulation. Adv Photo Res 2000103. https://doi.org/10.1002/adpr.202000103

Vurro, V., Venturino, I., Lanzani, G., 2022. A perspective on the use of light as a driving element for bio-hybrid actuation. Appl. Phys. Lett. 120, 080502. https://doi.org/10.1063/5.0078411

Zhang, J., Wang, J., Tian, H., 2014. Taking orders from light: progress in photochromic bio-materials. Mater. Horiz. 1, 169–184. https://doi.org/10.1039/C3MH00031A

Supplementary to:

Optical modulation of excitation-contraction coupling in human induced pluripotent stem cell-derived cardiomyocytes

Vito Vurro, Beatrice Federici, Carlotta Ronchi, Valentina Sesti, Silvia Crasto, Claudia Maniezzi, Maria Rosa Antognazza, Chiara Bertarelli, Elisa Di Pasquale, Guglielmo Lanzani*, Francesco Lodola*

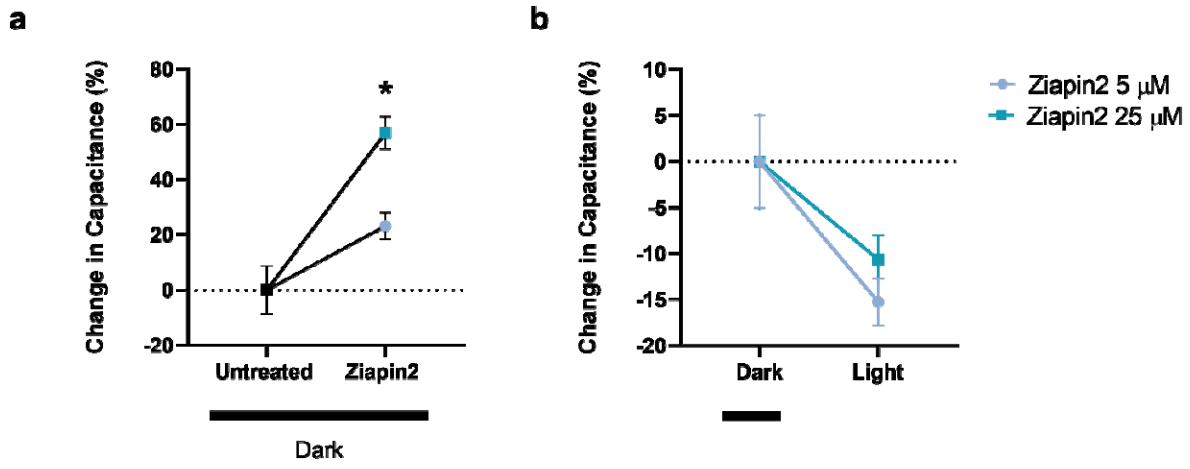

Figure S1. Ziapin2-mediated modulation of membrane capacitance. *Evaluation of capacitance changes in hiPSC-CMs upon Ziapin2 internalization* ***(panel a)*** *and photoisomerization* ***(panel b)****. Ziapin2 5μM represented with light blue dots while 25 μM in teal squares. Light power density, 80 mW/mm^2. The experiments were carried out at room temperature (24°C). n = 15 and 20 for untreated and Ziapin2-loaded cells respectively from three independent differentiations. Data are represented as mean ± sem.*

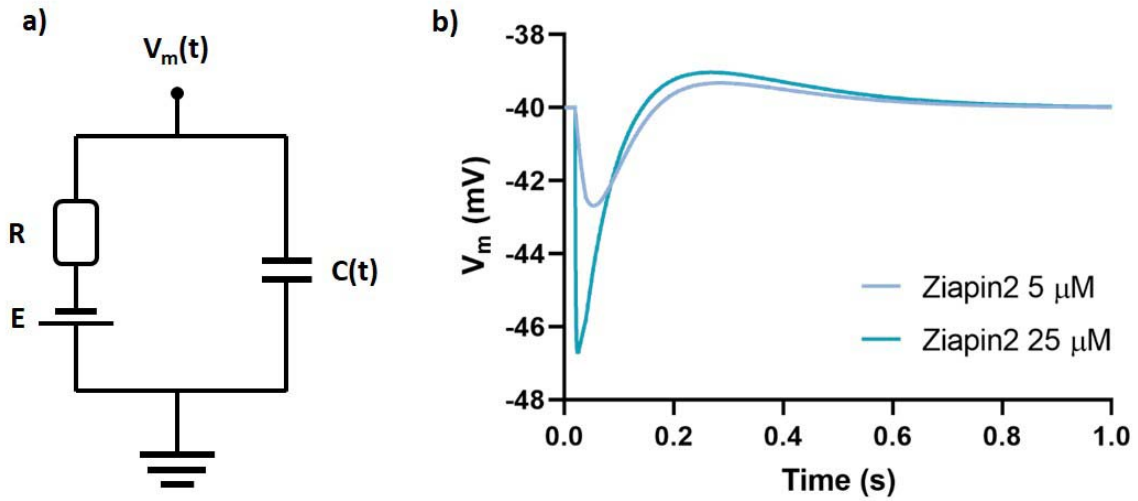

Figure S2. Simulation of membrane voltage. *Simulated equivalent circuit (**panel a**) and capacitance-induced membrane potential variation (**panel b**). This simulation, performed as previously described* (DiFrancesco et al., 2020)*, mimicks the effect of a 20 ms light pulse on Ziapin2 photoisomerization (a capacitance variation) and subsequent membrane potential modulation. In order to reproduce the observed effect, only the photoisomerization characteristic time has been reduced (t_{hyp} = 35ms for 5mM and t_{hyp} = 1ms for 25mM). This could be consistent with the localization of Ziapin2 in membrane domains more prone to favour isomerization.*

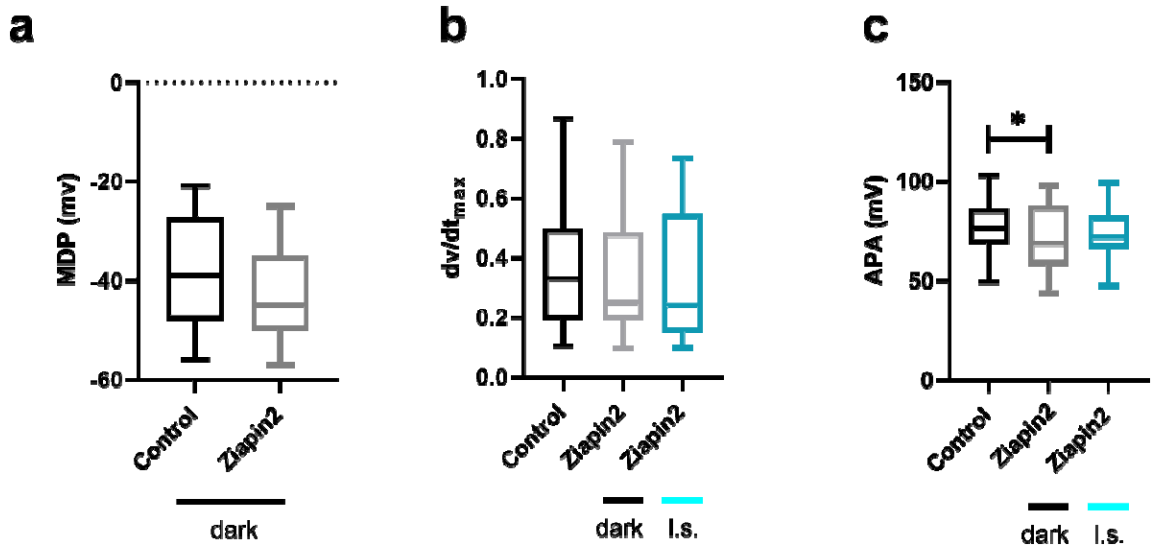

Figure S3. AP parameters in hiPSC-CMs exposed to Ziapin2. *Comparison of the maximum diastolic potential (MDP,* ***panel a****), maximal rate of rise (dv/dt$_{max}$,* ***panel b****) and AP amplitude (APA,* ***panel c****) between spontaneous and light-evoked APs in 25µM Ziapin2 loaded hiPSC-CMs (n > 40 for each condition from three independent differentiations). Data are presented as box and whiskers plot (min to max). Light power density, 80 mW/mm^2. The experiments were carried out at room temperature (24°C). * p < 0.05.*

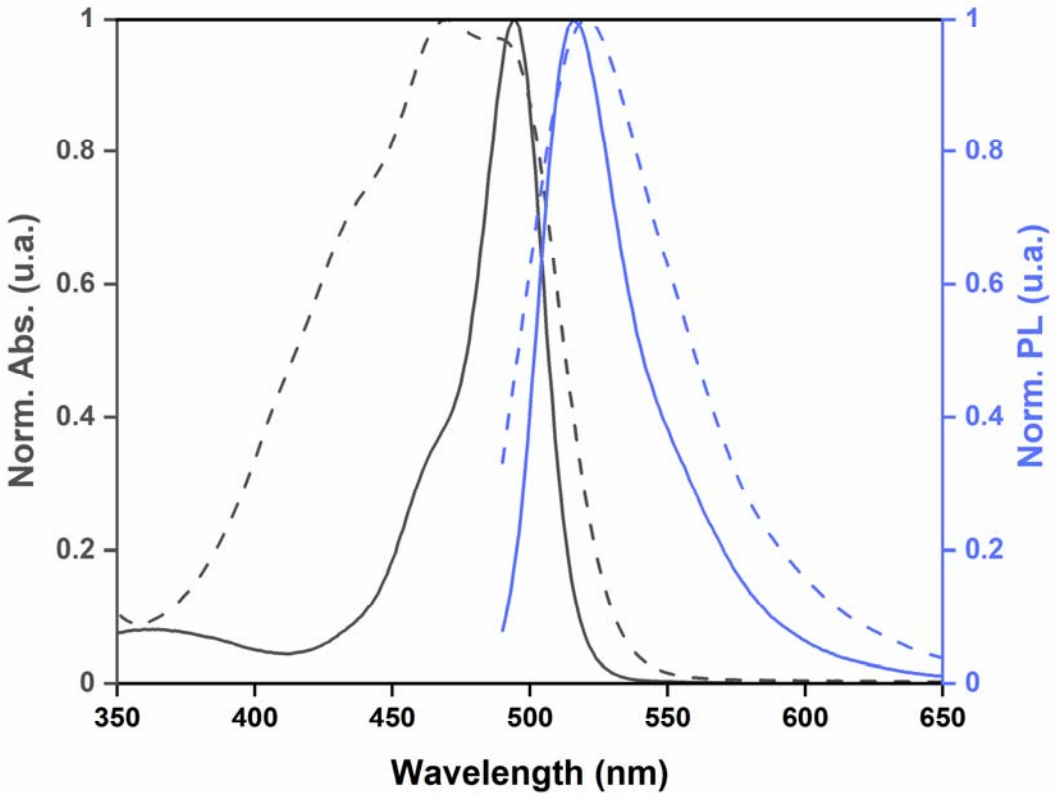

Figure S4 – *Fluorescence emission and excitation spectra of Ziapin2 and Fluo-4 AM.* *Normalized UV-vis absorption (Norm. Abs., grey) and photoluminescence (Norm. PL, blue) spectra of Fluo-4 AM (solid line) and Ziapin2 (dashed line).*

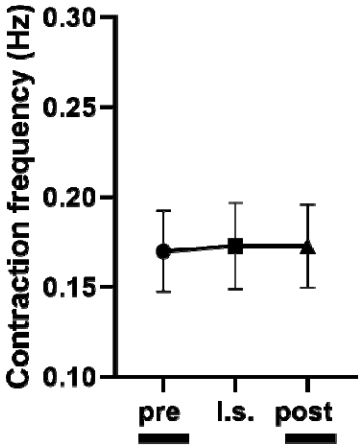

Figure S5. Light-induced contraction rate modulation in hiPSC-CMs incubated with vehicle. *DMSO-treated hiPSC-CMs contraction frequency before (pre), during (l.s.), and after (post) 1 Hz pulsed light stimulation at light power density = 30 mW/mm^2 (n = 25 from three independent differentiations, data are shown as mean ± sem). The experiments were carried out at room temperature (24°C).*